Lawrence Berkeley National Laboratory

Title

Influence of the Sb dopant distribution on far infrared photoconductivity in Ge:Sb blocked impurity band detectors

Permalink

https://escholarship.org/uc/item/65g6x6bj

Authors

Bandaru, Jordana
Beeman, Jeffrey W.
Haller, Eugene E.
et al.

Publication Date

2002-02-06

Peer reviewed

7Influence of the Sb dopant distribution on far infrared photoconductivity in Ge:Sb Blocked Impurity Band detectors

Jordana Bandaru[+a,b], Jeffrey W. Beeman[b], Eugene E. Haller[*a,b]

[a]University of California, Berkeley and [b]Lawrence Berkeley National Laboratory,
Berkeley, CA 94720

Stacy Samperi and Nancy M. Haegel
Department of Physics, Fairfield University, Fairfield, CT 06430

Extended long wavelength response to ~200 μm (50 cm^{-1}) has been observed in Ge:Sb Blocked Impurity Band (BIB) detectors with N_D ~ 1 x 10^{16} cm^{-3}. The cut-off wavelength increases from 150 μm (65 cm^{-1}) to 200 μm (50 cm^{-1}) with increasing bias. The responsivity at long wavelengths was lower than expected. This can be explained by considering the observed Sb diffusion profile in a transition region between the blocking layer and active layer. BIB modeling is presented which indicates that this Sb concentration profile increases the electric field in the transition region and reduces the field in the blocking layer. The depletion region consists partially of the transition region between the active and blocking layer, which could contribute to the reduced long wavelength response. The field spike at the interface is the likely cause of breakdown at a lower bias than expected.

1. INTRODUCTION

The far infrared region of the electromagnetic spectrum (25-200 μm or 50-400 cm^{-1}), still largely unexplored, is of great interest to astronomers, astrophysicists, and cosmologists [1,2,3]. The development of sensitive far infrared detectors will enable the study of scientific phenomena such as the birth and evolution of planetary systems. Ge:Ga and Ge:Sb photoconductors have been the state-of-the-art for the 50-130 μm (77-200 cm^{-1}) region for both high-background balloon and airplane-based observations as well as low background satellites where detector dark current must be minimal. In order to reach wavelengths longer than 130 μm (77 cm^{-1}), a uniaxial compressive stress is applied to Ge:Ga photoconductors,

extending the photoconductive response to 220 μm (45 cm^{-1})[4]. A 2 x 20 stressed Ge:Ga array will be flown on the Space Infrared Telescope Facility (SIRTF) to be launched in 2002. Germanium BIB detectors offer extended long wavelength response ($\geq$ 200μm or 50 cm^{-1}), and could potentially replace stressed Ge:Ga photoconductors as well as standard Ge photoconductors for far infrared astronomical observations. The Blocked Impurity Band (BIB) detector concept was first proposed in 1980 by Petroff and Stapelbroek at the Rockwell International Science Center [5]. Since then, BIB detectors implemented in silicon (e.g., Si:As and Si:Sb) have been successfully incorporated into infrared array cameras and spectrographs on satellites such as SIRTF [6]. The success of silicon BIB development is due in part to the large-scale efforts in growth of ultra-pure epitaxial silicon films. While growth of ultra-pure (<10^{10} cm^{-3}) bulk germanium crystals has been an important achievement [7], the growth of epitaxial layers of ultra-pure Ge has not been well established. The development of a growth process for achieving pure epitaxial Ge layers is essential to the realization of Ge BIB detector arrays.

A schematic of an n-type BIB detector is shown in Figure 1a. The device is comprised of two semiconducting layers, a pure blocking layer and a doped infrared (IR) absorbing layer which serves as the active layer of the device. The two layers are sandwiched between degenerately doped contacts. The active layer is doped near the metal insulator transition such that an impurity band is formed. This both lowers the minimum detectable photon energy and increases the linear optical absorption coefficient [8,9]. A BIB device can therefore achieve extended long wavelength response with a volume of active material ~ 100 times smaller than a traditional photoconductor. This is important since a smaller device is less susceptible to interference from cosmic radiation. Impurity banding in the active layer necessitates a pure blocking layer to prevent unacceptably large dark current. The operating principle of an n-type BIB detector is illustrated in Figure 1b. The active layer contains a high concentration of n-type dopant (~ 10^{16} cm^{-3} for Ge) and a residual compensating p-type dopant (~ 10^{12} cm^{-3} for Ge). Under reverse bias, electrons move in the impurity band toward the positive contact and are stopped by the blocking layer. Ionized donor states are filled in leaving behind a region of negative space charge created by ionized acceptor states. This region is the depletion layer of width w, and it depends on applied bias (V_a), acceptor concentration (N_A), and blocking layer thickness (b) as determined by Petroff and Stapelbroek:

$$w = \left[\sqrt{\frac{2\varepsilon\varepsilon_0 (V_a - V_{bi})}{eN_A} + b^2} \right] - b \tag{1}$$

where $\varepsilon\varepsilon_0$ is the dielectric constant, e is the electron charge, and V_{bi} is the built-in potential which is small and can be neglected. The depletion layer is the active region of the device. A large depletion width requires N_A and b to be small.

A numerical finite difference model has been developed to calculate realistic field profiles in BIB devices with a wide range of material properties [10]. Space charge effects and spatial doping variations are taken into account. Modeling has focused on p-type Ge:Ga BIB structures, but has been extended to Ge:Sb in this work. The doping requirements for the blocking layer can be better understood by modeling. Ge photoconductors typically contain ~ 10^{14} cm^{-3} shallow dopants without incurring significant dark currents. Modeling has shown that the electric field distribution in the BIB blocking layer is highly non-uniform at these levels and can affect field penetration in the active layer. The diffusion of dopants at the blocking/active layer interface is also shown to be important and will be discussed further.

Previous efforts to grow germanium BIB structures by chemical vapor deposition (CVD) of Ge:Ga [11,12] showed response down to 50 cm^{-1}, however results were not reproducible and the detectors suffered from large dark currents due to unpassivated surfaces. Epilayers of pure Ge were grown on bulk doped substrates which served as the active layer. This structure contributed to a high series resistance and slowed down the devices considerably. Epitaxial growth of both the pure and active layers would eliminate this problem. Liquid phase epitaxy was chosen for its potential as a high purity technique with the ability to grow layers 1-100 μm thick. Preliminary results were encouraging showing some extended wavelength response [13]. LPE growth takes place as the growth materials precipitate out of a low melting point solution. Most impurities preferentially segregate to the liquid phase rather than the solid epilayer, and segregation coefficients of 10^{-2}-10^{-3} are common (e.g. As, Sb, Bi for Ge grown from Pb solution). Lead was chosen as a solvent because it is isoelectronic with Ge, has a low melting point, and has a low solubility in Ge. The purity of commercially available Pb was found to be a problem, with n-type impurities ~ 10^{15} cm^{-3}, identified by photothermal ionization spectroscopy to be phosphorus. The current work focuses on Sb dopant distribution in BIB devices fabricated by growth of heavily doped epilayers on pure substrates.

2. EXPERIMENTAL PROCEDURES

A. Liquid Phase Epitaxy

Epitaxial layers of Sb-doped Ge were grown from a Pb solvent by Liquid Phase Epitaxy in a tipping boat system. Pure Ge substrates (n=2×10^{12} cm^{-3}) oriented to within 0.01° of the <111> were chosen as blocking layer material. Ge

substrates 8x8x0.5 mm^3 were held by a graphite clip in a graphite crucible loaded into a single zone quartz tube furnace. LPE growth was carried out in 1 1/3 atm palladium diffusion purified H$_2$. The Sb dopant concentration was controlled by addition of a Pb-Sb alloy to ~ 10g of 6N pure Pb solvent. Typical Sb-doped layers contained ~ 10^{16} cm^{-3} Sb. The solvent was saturated with ultra-pure Ge at 655 °C and equilibrated for 5.5 hours. The system was tipped at an undercooling of 3 °C to begin growth. Layer growth occurred as the furnace temperature was ramped down to 340 °C over 12 hours. A typical epilayer thickness is 40 μm.

B. Blocked Impurity Band detector fabrication

Because of the difficulty in obtaining pure Pb, an Sb-doped active layer was grown on a pure substrate which was then thinned down to form the blocking layer. A schematic of a BIB device structure is shown in Figure 2. In order to achieve a thicker final device (for mechanical stability purposes), a double layer was grown. The top 10 μm were polished off of the first layer before growing a second layer, and the surface of the second layer was polished as well for reasons described in the following section. After polishing the epilayer, the surface was implanted with phosphorus ions (2 x 10^{14} cm^{-2} at 40 kV and 4 x 10^{14} cm^{-2} at 100 kV) at 77K. The sample was diced into rectangular pieces of 3 mm x 2.5 mm for easier handling when thinned. The substrate was then lapped and polished to leave a 10 μm thick blocking layer. The pure side was masked around the edges with picene wax and phosphorus ions were implanted (2 x 10^{14} cm^{-2} at 33 kV) into this masked surface. Implanted samples were annealed at 450 °C for 2 hours in flowing Ar gas before metallization. After annealing, 200Å Pd/4000 Å Au were sputter deposited onto both sides of the device. A finger structure was painted on the pure side with picene wax, and was used as a mask for the Pd/Au deposition. The finger structure was used to leave ~1/3 of the implanted surface area transparent to IR while still applying a relatively uniform electric field to the device.

C. Blocked Impurity Band detector modeling

Steady state spatial electric field distributions in the absence of light have been calculated using a numerical finite difference approach as described in reference 10. The relevant parameters are defined below:

Blocking layer thickness	20 µm
Blocking layer doping	$N_D = 2 \times 10^{12}$ cm^{-3}, $N_A = 1 \times 10^9$ cm^{-3}
Active layer doping	$N_D = 1 \times 10^{16}$ cm^{-3}, $N_A = 2 \times 10^{12}$ cm^{-3}
Bias	30 mV
Temperature	2.5 K
Electron mobility in the blocking layer	3×10^6 cm^2/Vs
Bohr radius for Ge:Sb	37×10^{-8} cm

Gradients in Sb concentration (N) across the interface have been considered, and are defined by a grade parameter (g) as follows:

$$N = N_1 + \frac{(N_2 - N_1)}{1 + \exp[(a - x)/g]} \tag{2}$$

where N_1 and N_2 are the layer dopings, a is the interface position, and x is the position variable.

3. RESULTS AND DISCUSSION

A. Sb distribution in the active layer

The distribution of Sb in doped Ge LPE layers had to be determined accurately due to its potential effect on photon absorption and electric field profiles in a BIB device. Spreading resistance measurements on angle-lapped Sb doped layers (Figure 3) revealed a highly doped surface region of a few microns in thickness. This surface region was formed at the lowest growth temperatures in the cooling cycle. At low temperatures Sb cannot diffuse rapidly enough away from the growth interface increasing the effective segregation coefficient leading to a sharp increase in near-surface Sb concentration.

Therefore, for all Hall effect and detector measurements in this work, 10 μm have been removed from the surface of all doped layers by chemomechanical polishing (CMP) or chemical etching using a 20:1 HNO$_3$:HF mixture. A transition region between the substrate and epilayer was observed in the spreading resistance measurements. Because of the possibility that the transition region could be an artifact due to the finite probe diameter in spreading resistance, Secondary Ion Mass Spectroscopy (SIMS) was used to study this transition region in finer detail. SIMS data given in Figure 4a shows significant Sb diffusion into the ultra-pure Ge substrate (blocking layer). The concentration drops an order of magnitude over ~1.5 μm. This observation is supported by diffusivity data [14]. The diffusivity of Sb in Ge at 650 °C is 4 x 10^{-13} cm^2/s. The temperature ramps down during growth, however an estimate of $\sqrt{Dt}$ at 650°C for 2 hours is 0.8 μm.

It is interesting to compare the diffusion behavior of Sb and Ga in Ge. For Ga in Ge the diffusivity at 650 °C is 9 x 10^{-17} cm^2/s. For a growth cycle starting at 650 °C, Ga would diffuse only 8 nm. Unfortunately, the presence of n-type dopants in the Pb solvent prevents the fabrication of p-type devices at this time. A study of devices grown at low temperature would be interesting as well. An Sb-doped layer grown at 550 °C shows a sharp interface with no observable diffusion as seen in Figure 4b. However, layers grown at low temperatures are generally only ~ 10 μm thick, including the region of high Sb concentration at the surface. Although enough Ge is present in the melt to obtain thicker films, many nucleation sites have been observed in the Pb melt after growth. Nucleation at these secondary sites limits the amount of Ge available for growth. The origin of the secondary nucleation sites is still under investigation. Alternate methods for obtaining thicker films at low temperatures are currently under consideration.

SIMS data have also indicated oxygen and carbon at the original growth interface, the effects of which on a device are not known. A study is currently underway to eliminate such a layer by meltback of the surface before growth.

The observed diffusion profile is expected to have several effects on BIB performance. Figure 5 shows the results of simulations of the E-field distribution across a BIB detector with 30 mV applied bias. Figure 5a shows the E-field distribution for a sharp interface (g=8x10^{-7} cm). The Sb profile in our LPE layers corresponds to the grade parameter g=6x10^{-5} cm shown in Figure 5b. The high field at the interface is expected to enhance device breakdown at smaller applied bias. The depletion width of the device would consist partly of material doped to some intermediate value between the blocking layer and the active layer. This material would have a narrower impurity band giving rise to a reduced long wavelength response in the transition region. In addition, the extreme diffusion of Sb into the blocking layer would reduce its

blocking effectiveness. It should be noted that the simulations represent a 20 µm thick blocking layer whereas our devices have a 10 µm thick blocking layer. The profiles are therefore similar to those of a 15 mV bias across a 10 µm blocking layer.

B. Blocked Impurity Band detector characterization

An Sb doped germanium layer ~ 1 x 10^{16} cm^{-3} grown at 650°C was used to fabricate a BIB detector as described above. The current – voltage behavior of this detector at 2 K is shown in Figure 6. Under positive bias (reverse bias for an n-type BIB) the device is blocking. It begins to break down at ~ 40 mV. Under negative bias the device behaves like a forward biased diode. Under positive bias below 40 mV the leakage current is below 10^{-14} A, the detectability limit of our electronics. The spectral response of this Ge:Sb BIB at 2K is shown in Figure 6 for three different applied bias values. Fabry-Perot oscillations are present at regularly spaced intervals ~ 40 cm^{-1} apart (e.g. maxima occur at ~ 80 cm^{-1} and ~ 120 cm^{-1}) which corresponds to 30 µm of germanium. The sample is close to this thickness so it is thought that the intensity oscillations are likely to originate inside the sample. The Fabry-Perot oscillation pattern is more clearly distinguishable when the spectrum is extended to high frequency. For Sb-doped Ge the peak response is ~ 100 cm^{-1} which falls on a Fabry-Perot minimum in this sample. For reference, the strongest photothermal peak for Sb in Ge occurs near 69.5 cm^{-1} at T= 2K. The peak observed in this region of the spectrum is the corresponding broadened photothermal peak. Long wavelength response is observed compared to a standard Ge:Sb photoconductor. It can be seen that the onset of photoconductivity extends to lower wavenumbers (longer wavelength) as the bias is increased. This may be the effect of the E-field on the excited states, or it could be understood by considering the depletion in the active layer of the BIB. Since there is a transition region between the pure substrate and the Sb-doped layer due to Sb diffusion during growth, the material being depleted at low applied bias will contain less Sb than the material depleted at high applied bias. A critical consequence of the Sb gradient is that the device breaks down at a lower bias than expected due to the high field at the interface.

The minority dopant concentration in the active layer, which determines the BIB depletion width, was determined to be ~ 2x10^{12} cm^{-3} by variable temperature Hall effect measurements. Unintentionally doped layers were used since heavily doped layers undergo hopping conduction at low temperatures. Direct determination of N_A on a detector structure can be accomplished by capacitance vs. voltage measurements using a two-phase lock-in amplifier. Combining equation 1 along with the capacitance (C) of a BIB under positive bias:

$$C = \frac{\varepsilon\varepsilon_0 A}{w + b}$$

(3)

the acceptor concentration (N_A) can be determined from the slope of $1/C^2$ vs. V. Preliminary C-V results agree with variable temperature Hall effect measurements on unintentionally doped LPE layers. However, interpretation of the C-V data is not straightforward due to the effect of the transition region on the electric field profile. With a $10\,\mu m$ blocking layer the depletion width of the device is ~ $1.5\,\mu m$ at 40 mV bias using equation 1. It should be noted that the depletion width calculated here does not take into account the Sb diffusion profile. As can be seen in Figure 5, the presence of the gradient increases the size of the depletion width beyond what is expected for a sharp interface.

4. CONCLUSIONS

Extended long wavelength response which increases with bias has been observed in Ge:Sb BIB detectors. A significant Sb concentration gradient in the transition region between the blocking layer and active layer was observed using SIMS. BIB modeling indicates that the Sb gradient would increase the electric field in the transition region and reduce the field in the blocking layer. In addition, the depletion region would be larger than that calculated with a sharp Sb gradient. The depleted material would consist partly of the transition region between the active and blocking layer. This material would be doped lower than the bulk layer and may contribute to the reduced long wavelength response. The elimination of the transition region would be expected to improve the blocking ability of the device significantly, and should allow the device to withstand higher bias. With the development of Sb-doped layers grown at lower temperatures, we are hopeful that Ge BIB detectors will obtain the expected significant long wavelength response.

ACKNOWLEDGEMENTS

[1] D. Lemke, M. Stickel, K. Wilke (Eds.), *ISO Surveys of a Dusty Universe* (Springer-Verlag, Germany, 2000).

[2] G. Pilbratt, Infrared Phys. Technol., **35**, (2/3), 407 (1994).

[3] G.H. Rieke, M.W. Werner, R.I. Thompson, E.E. Becklin, W.F. Hoffmann, J.R. Houck, F.J. Low, W.A. Stein, F.C. Witteborn, Science, **231**, 807 (1986).

[4] E.E. Haller, M.R. Hueschen, P.L. Richards, Appl. Phys. Lett., **34**, 495 (1979)

[5] M.D. Petroff, M.G. Stapelbroek, U.S. Patent No. 4568960.

[6] G.H. Rieke, in *ISO Surveys of a Dusty Universe*, Proceedings of a Ringberg Workshop held at Ringberg Castle, Tegernsee, Germany, 8-12 November 1999, edited by D. Lemke, M. Stickel, K. Wilke, 394 (Springer-Verlag, Germany, 2000).

[7] E.E. Haller, W.L. Hansen, F.S. Goulding , Advances in Physics, **30** (1), 93 (1981).

[8] Y. Nisida and K. Horii, J. Phys. Soc. Jap., **26** (2) , 388 (1969).

[9] J. Bandaru, J. Beeman, E. Haller, Submitted to Appl. Phys. Lett. for publication.

[10] N.M. Haegel, J.E. Jacobs, A.M. White, Appl. Phys. Lett., **77**(26), 4389 (2000).

[11] D.M. Watson, M.T. Guptill, J.E. Huffman, T.N. Krabach, S.N. Raines, S. Satyapal, J. Appl. Phys., **74**(6), 4199 (1993).

[12] J.E. Huffman, N.L. Casey, J. Crystal Growth, **129**, 525 (1993).

[13] C.S. Olsen, J.W. Beeman, W.L. Hansen, E.E. Haller, in *Infrared Applications of Semiconductors II. Symposium, Boston, MA, 1-4 Dec. 1997*, edited by D.L. McDaniel, Jr.et al., Mat. Res. Soc. Proc., **484**, 215 (1998).

[14] N.A. Stolwijk, H. Bracht, in *Landolt Boernstein, New Series, Vol. III/33, Diffusion in Semiconductors and Non-Metallic Solids*, edited by D. L. Beke, Subvolume A: Diffusion in Semiconductors (Springer, Berlin, 1998).

Figure Captions

Figure 1. (a) Schematic of an n-type Blocked Impurity Band detector and (b) band diagram shown for a device with an electric field applied. Heavily doped contacts are labeled n^{++}. D^+ = ionized donor, D^0 = neutral donor, A^- = ionized acceptor, w = depletion width.

Figure 2. Schematic of BIB device structure (not to scale). A thin layer of phosphorus implanted Ge which is IR transparent is indicated in light gray on the top surface.

Figure 3. Free electron concentration vs. depth for an Sb doped Ge LPE layer grown at 655 °C as determined by spreading resistance measurements. TR indicates the transition region. Bulk calibration standards of known concentration were used to convert the spreading resistance to resistivity. An average constant mobility determined from three standards (concentrations 8.6 x 10^{16}, 2.0 x 10^{16}, and 5.3 x 10^{14} cm^{-3}) was used for converting resistivity to electron concentration. The concentration of the substrate appears higher than its actual value because the spreading resistance vs. resistivity no longer follows the curve fit in this region. The actual concentration in the substrate is below intrinsic.

Figure 4. Concentration vs. depth obtained by SIMS analysis with a Cs ion beam for (a) Sb, O, and C in a Ge LPE layer grown at a starting temperature of 650 °C on a pure Ge substrate. Oxygen and carbon are observed at the layer-substrate interface. The profile after ~ 5 μm is limited by the instrument resolution (~ 10^{16} cm^{-3}). (b) Sb in a Ge layer grown at 550 °C. The measurement in the substrate is limited by the instrument resolution. LPE layers have been polished prior to SIMS in order to probe only the region near the substrate. SIMS sputter rate = 58 Å/sec

Figure 5. Model of electric field distributions for 30 mV applied bias and Sb concentration gradients across the blocking layer/active layer for (a) a sharp gradient, g= 8x10^7 cm and (b) a gradient similar to that observed in epilayers grown at 650 °C, g=6x10^5 cm . The interface is at 35 μm.

Figure 6. (a) Dark current – voltage characteristics of a Ge:Sb BIB detector at 2 K. At 0 bias the dark current is below the detection limit for the electronics.(b) Spectral response of the BIB detector at 2 K with increasing applied bias. The inset shows an enlargement of the long wavelength onset in photoconductive response and its extension with applied bias.
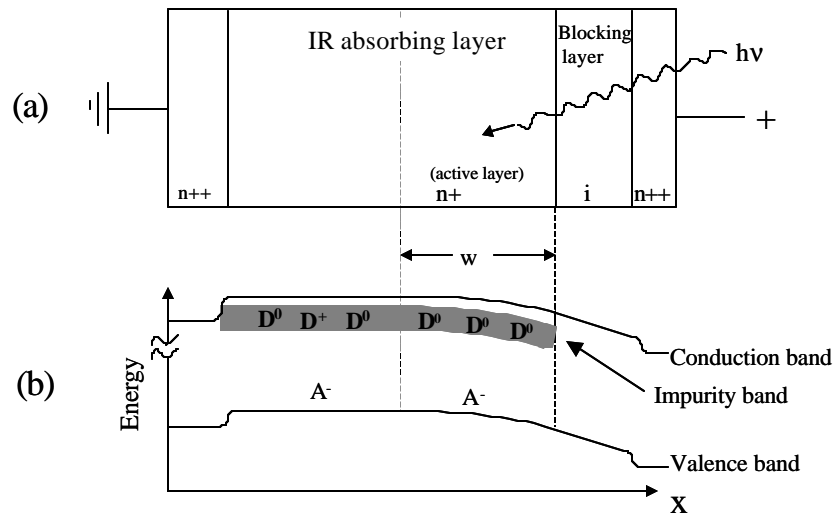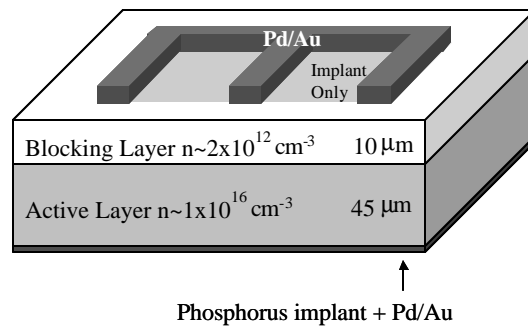
(a)

IR absorbing layer

Blocking
layer

hν

+

(active layer)

n++

n+

i

n++

w

(b)

Energy

D⁰ D⁺ D⁰   D⁰ D⁰ D⁰

A⁻   A⁻

Conduction band

Impurity band

Valence band

X

Figure 1
J. Bandaru et al.

Pd/Au

Implant
Only

Blocking Layer n~2×10^{12} cm^{-3} 10 μm

Active Layer n~1×10^{16} cm^{-3} 45 μm
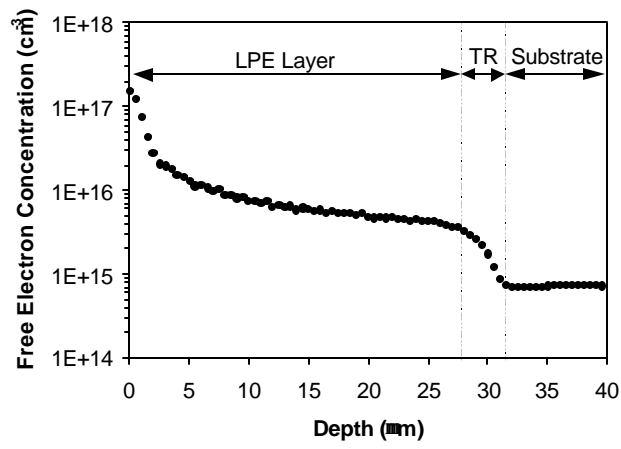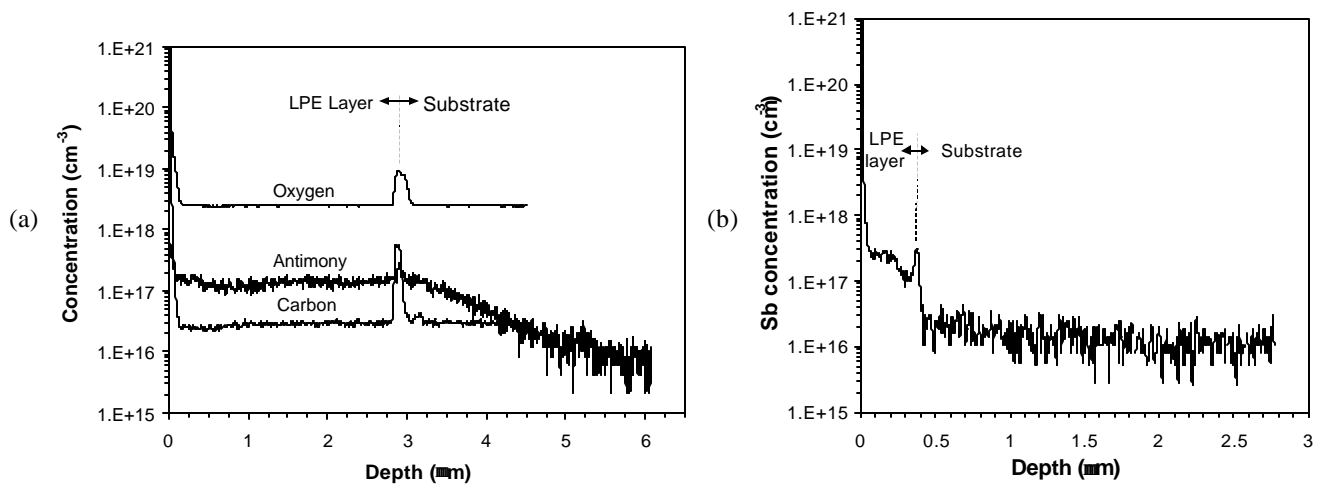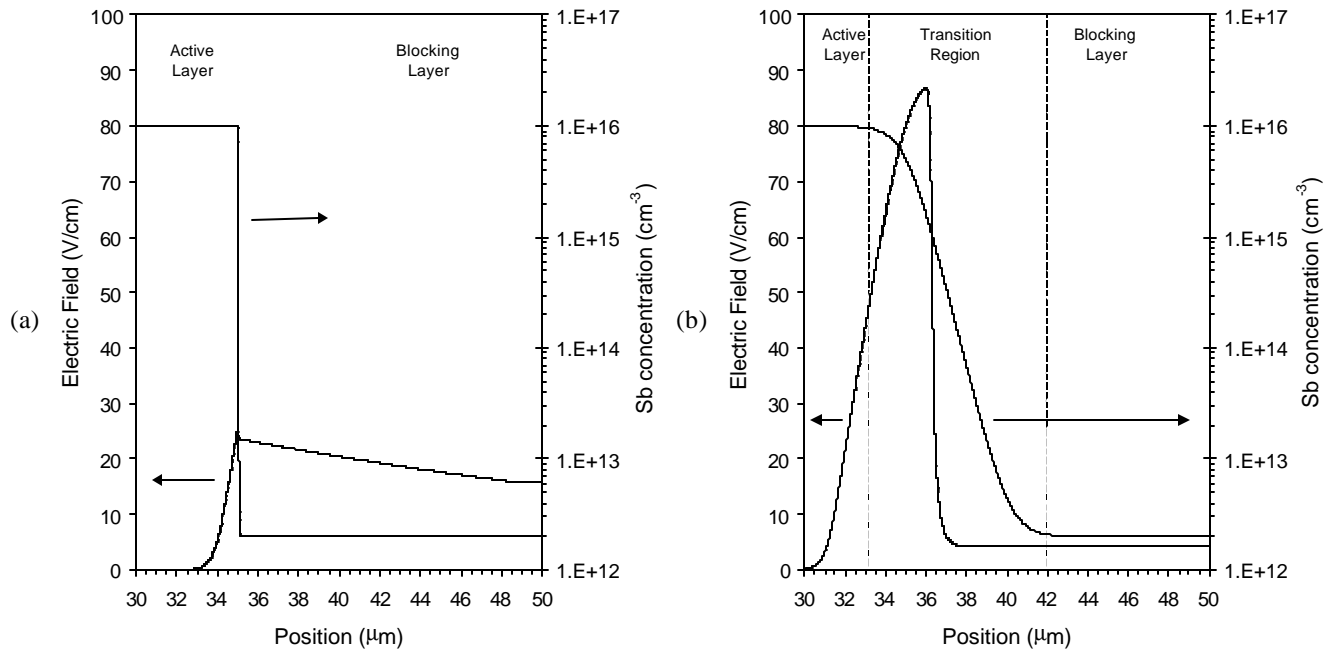
Phosphorus implant + Pd/Au

Figure 2
J. Bandaru et al.

Figure 3
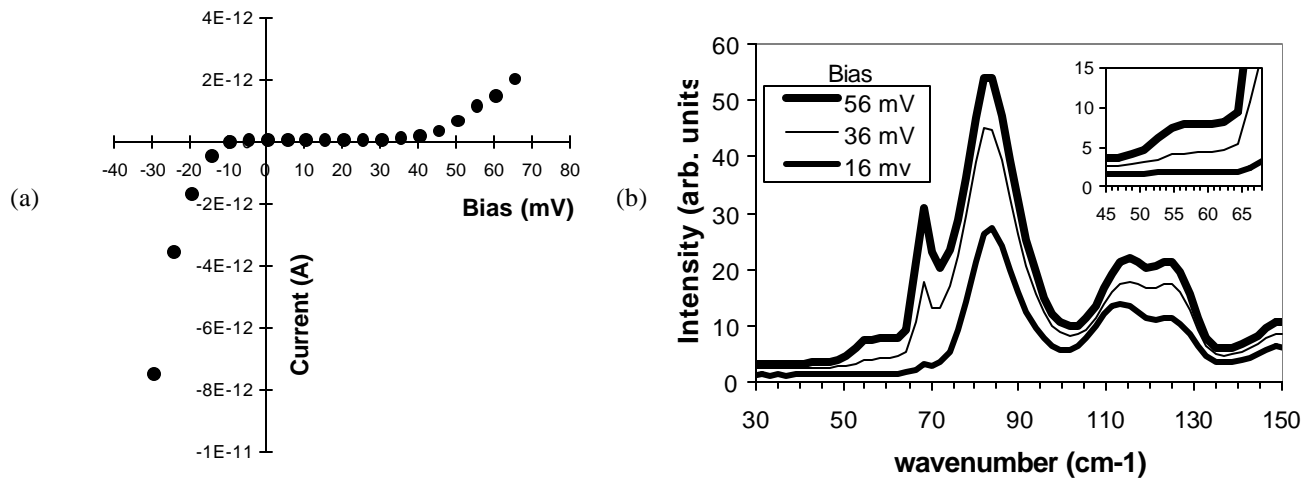J. Bandaru et al.

(a)

(b)

Figure 4
J. Bandaru et al.

Figure 5
J. Bandaru et al.

(a)

(b)

Figure 6
J. Bandaru et al.